Contents:

The methods for determinations of the dissociation rate (k_d) of $Ta_3N_2C_2H_2^-$ → TS6 → I6 and the collision rate of $Ta_3N_2C_2H_2^-$ with the cooling gas He ($k_{collision}$).

The Rice-Ramperger-Kassel-Marcus (RRKM) theory calculations are performed to estimate the dissociation rate (k_d) of $Ta_3N_2C_2H_2^-$ → **TS6** → **I6** by using the following equation[1]:

$$k(E) = N^{\neq}(E - E^{\neq}) / \rho(E) / h \quad (1)$$

in which $\rho(E)$ denotes the density of states of the meta-stable intermediates at the energy E [= E_1 (binding energy of $Ta_3N_2C_2H_2^-$) + E_2 (vibrational energy of $Ta_3N_2C_2H_2^-$) + E_3 (center-of-mass collisional energy], $N^{\neq}(E - E^{\neq})$ is the total number of states of the transition state with a barrier $E^{\neq}$, and h is the Planck constant. E_1, E_2, $E^{\neq}$ and vibrational frequencies are all from the DFT calculations. In this system, the values of E_1, E_2, and E_3 are 2.77, 0.148, and 0.039 eV, respectively. Therefore, k_d is estimated to be 9.7×10^8 s^{-1}.

The effective pressure (P_2) of the cooling gas He is around 3.0 Pa in the ion trap.[2] The collision rate of $Ta_3N_2C_2H_2^-$ with He atoms is 6.9×10^5 s^{-1}, estimated by the following equation[3]:

$$k_{\text{collision}} = P_2 \sqrt{\frac{8\pi}{m_{\text{He}} k_{\text{B}} T}} (r_{\text{He}} + r)^2 \quad (2)$$

in which m_{He} is the mass of He atom, r_{He} is the van der Waals radius of He atom (1.40 Å), r is the radius of $Ta_3N_2C_2H_2^-$ (4.10 Å), k_B is the Boltzmann constant, and T is the temperature of the reactor. The radius of $Ta_3N_2C_2H_2^-$ is calculated by $r = (d_{N-H} + r_H + r_N)/2$, in which d_{N-H} is the distance between the N and the H atom (5.45 Å) in $Ta_3N_2C_2H_2^-$ and r_H (1.20 Å) and r_N (1.55 Å) are the van der Waals radii of H atom and N atoms, respectively.

Table S1. DFT-calculated and experimental bond dissociation energies. The values are in unit of eV.

	Methods	Ta–N	N–N	C–H	N–H
Experiment	Value	6.33±0.8	9.79± 0.01	3.51± 0.01	3.40 ± 0.16
	Reference			4	
Hybrid Functionals	**B3LYP**	**6.30**	**9.64**	**3.48**	**3.50**
	B1LYP	6.00	9.37	3.42	3.43
	B3P86	6.59	9.82	3.58	3.61
	B3PW91	6.34	9.47	3.41	3.41
	M05	6.68	9.40	3.44	3.36
	M052X	5.65	9.50	3.4	3.33
	PBE1PBE	6.26	9.45	3.37	3.37
	X3LYP	6.26	9.61	3.47	3.49
	M06	6.84	9.31	3.42	3.28
	M062X	6.01	9.48	3.38	3.29
	BHandHLYP	5.09	8.66	3.35	3.30
	BMK	6.08	9.53	3.39	3.39
Pure Functionals	BPW91	7.05	9.98	3.42	3.47
	BLYP	6.97	10.13	3.5	3.58
	BP86	7.25	10.29	3.6	3.69
	BPBE	7.07	9.98	3.41	3.46
	M06L	6.57	9.45	3.39	3.28
	PBE	7.25	10.27	3.46	3.53
	TPSS	6.73	9.57	3.57	3.60

Table S2. Wiberg bond orders of some important bonds in $Ta_3N_2^-$ and $Ta_3N_2C_2^-$ (shown in Figure 3) at B3LYP functional level.

	$Ta_3N_2^-$	$Ta_3N_2C_2^-$
N1–Ta1	1.4	1.4
N1–Ta3	1.3	1.4
N2–Ta2	1.5	1.4
N2–Ta3	1.2	1.4
Ta1–Ta2	2.2	0.6
Ta1–Ta3	1.6	0.3
Ta2–Ta3	0.8	0.3
C1–Ta1	–	1.7
C1–Ta2	–	1.7
C2–Ta1	–	1.2
C2–Ta2	–	1.2
C2–Ta3	–	1.2

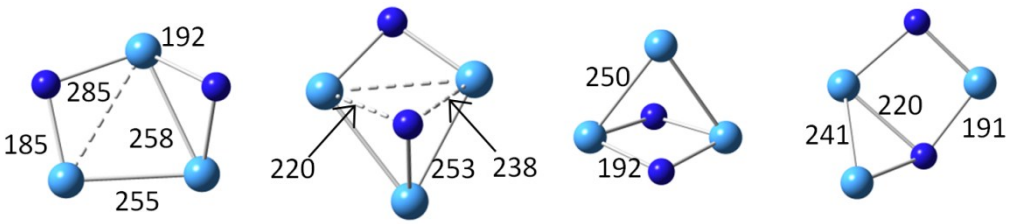

^{3}**IS1** $C_1/^3A$ 0.00	^{1}**IS2** $C_s/^1A'$ 0.27	^{3}**IS3** $C_s/^3A'$ 0.75	^{3}**IS4** $C_1/^3A$ 1.01
^{1}**IS1** $C_1/^1A$ 0.35	^{3}**IS2** $C_s/^3A'$ 0.41	^{1}**IS3** $C_s/^1A'$ 0.89	^{1}**IS4** $C_1/^1A$ 1.28
^{5}**IS1** $C_1/^5A$ 0.64	^{5}**IS2** $C_s/^5A'$ 1.13	^{5}**IS3** $C_s/^1A'$ 1.28	^{5}**IS4** $C_1/^5A$ 1.47

Fig. S1: DFT-calculated structures and relative energies of $Ta_3N_2^-$. The point group and electronic state are given under each structure. Some bond lengths are given in pm. The superscripts indicate the spin states.

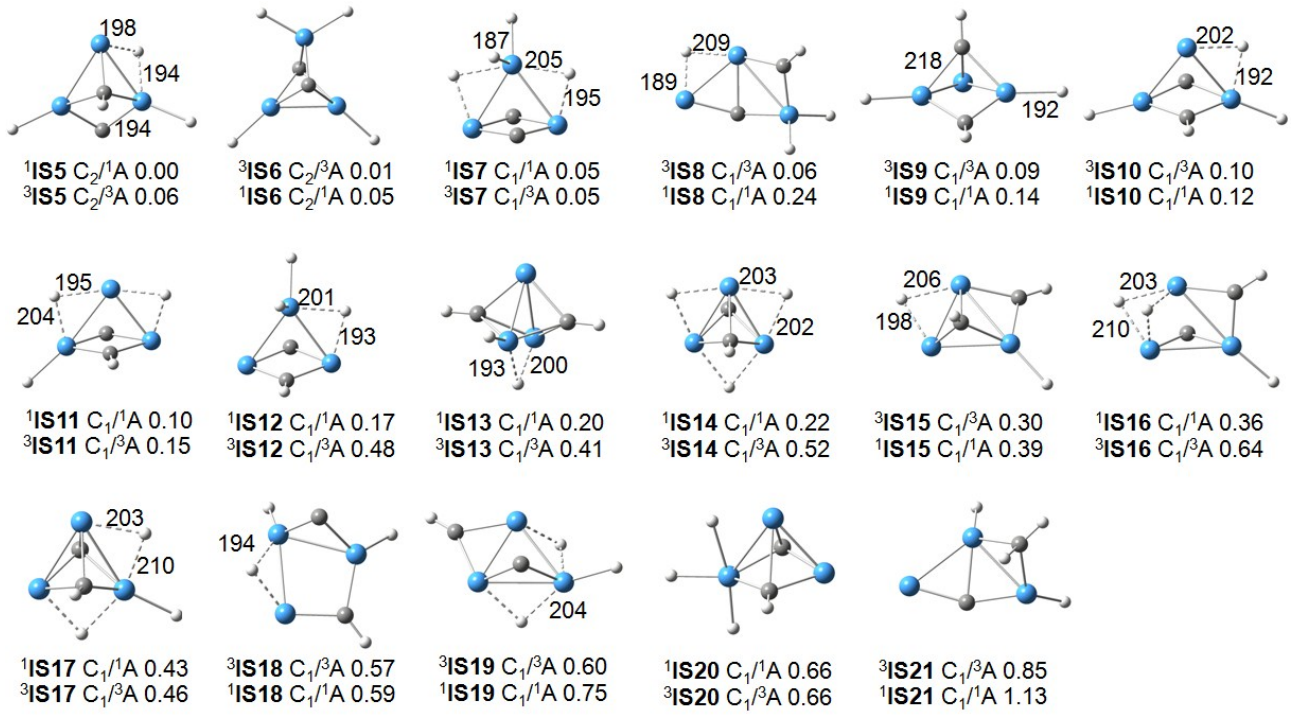

^{1}**IS5** $C_2/^1A$ 0.00
^{3}**IS5** $C_2/^3A$ 0.06

^{3}**IS6** $C_2/^3A$ 0.01
^{1}**IS6** $C_2/^1A$ 0.05

^{1}**IS7** $C_1/^1A$ 0.05
^{3}**IS7** $C_1/^3A$ 0.05

^{3}**IS8** $C_1/^3A$ 0.06
^{1}**IS8** $C_1/^1A$ 0.24

^{3}**IS9** $C_1/^3A$ 0.09
^{1}**IS9** $C_1/^1A$ 0.14

^{3}**IS10** $C_1/^3A$ 0.10
^{1}**IS10** $C_1/^1A$ 0.12

^{1}**IS11** $C_1/^1A$ 0.10
^{3}**IS11** $C_1/^3A$ 0.15

^{1}**IS12** $C_1/^1A$ 0.17
^{3}**IS12** $C_1/^3A$ 0.48

^{1}**IS13** $C_1/^1A$ 0.20
^{3}**IS13** $C_1/^3A$ 0.41

^{1}**IS14** $C_1/^1A$ 0.22
^{3}**IS14** $C_1/^3A$ 0.52

^{3}**IS15** $C_1/^3A$ 0.30
^{1}**IS15** $C_1/^1A$ 0.39

^{1}**IS16** $C_1/^1A$ 0.36
^{3}**IS16** $C_1/^3A$ 0.64

^{1}**IS17** $C_1/^1A$ 0.43
^{3}**IS17** $C_1/^3A$ 0.46

^{3}**IS18** $C_1/^3A$ 0.57
^{1}**IS18** $C_1/^1A$ 0.59

^{3}**IS19** $C_1/^3A$ 0.60
^{1}**IS19** $C_1/^1A$ 0.75

^{1}**IS20** $C_1/^1A$ 0.66
^{3}**IS20** $C_1/^3A$ 0.66

^{3}**IS21** $C_1/^3A$ 0.85
^{1}**IS21** $C_1/^1A$ 1.13

Fig. S2: DFT-calculated structures and relative energies of $Ta_3C_2H_4^-$. The point group and electronic state are given under each structure. Some bond lengths are given in pm. The superscripts indicate the spin states.

$$Ta_3N_2^- + C_2H_4 \rightarrow Ta_3C_2H_4^- + N_2 \qquad (3)$$

The reaction 3 is thermally unavailable since it is endothermic. The zero-point vibration corrected energies (ΔH_{0K}) of this reaction is around 0.8 eV with respect to the separated reactants.

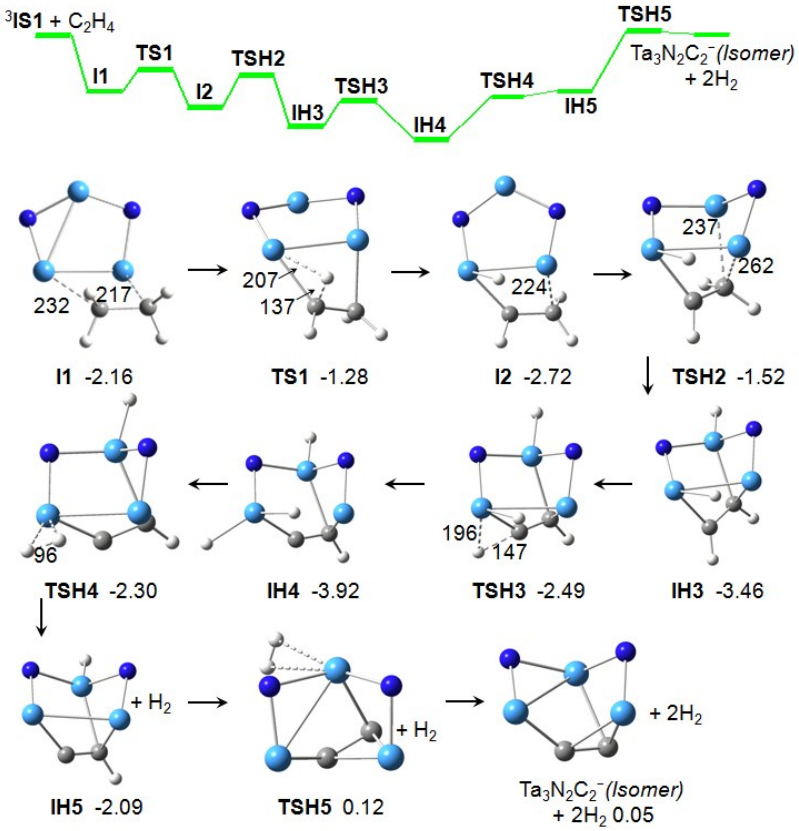

Fig. S3: DFT-calculated potential energy surface (PES) without C=C bond cleavage for the reaction of $Ta_3N_2^-$ with C_2H_4. The zero-point vibration corrected energies (ΔH_{0K} in eV) of the reaction intermediates, transition states, and products with respect to the separated reactants are given. The spin states are triplets.

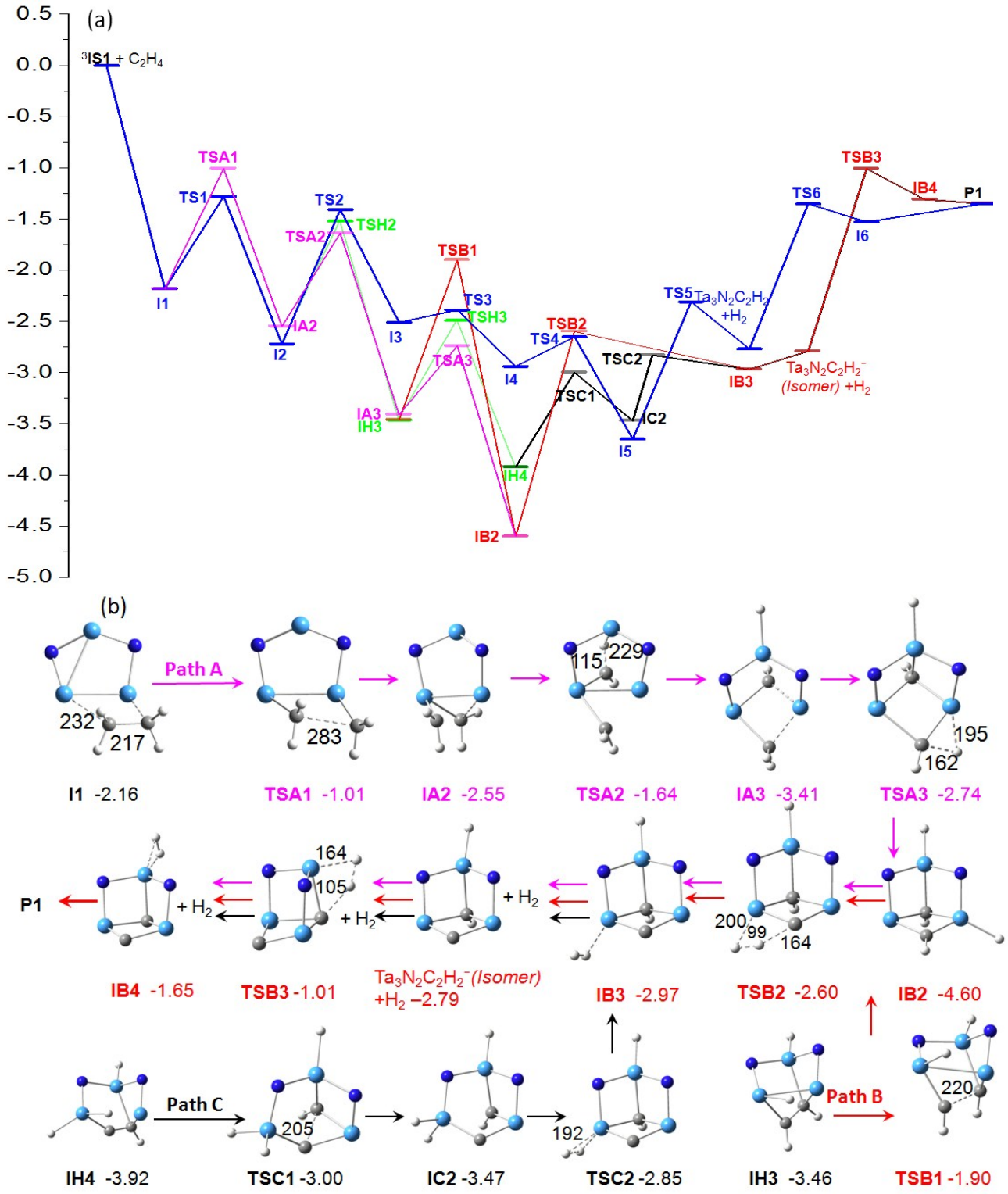

Fig. S4: DFT calculated other PESs to generate **P1**. Bond lengths are given in pm, and the spin states are triplets. The zero-point vibration corrected energies (ΔH_{0K} in eV) of the reaction intermediates, transition states, and products with respect to the separated reactants are given. The pathways in blue and in green are the ones shown in Fig. 3 of the main text and in Fig. S3, respectively.

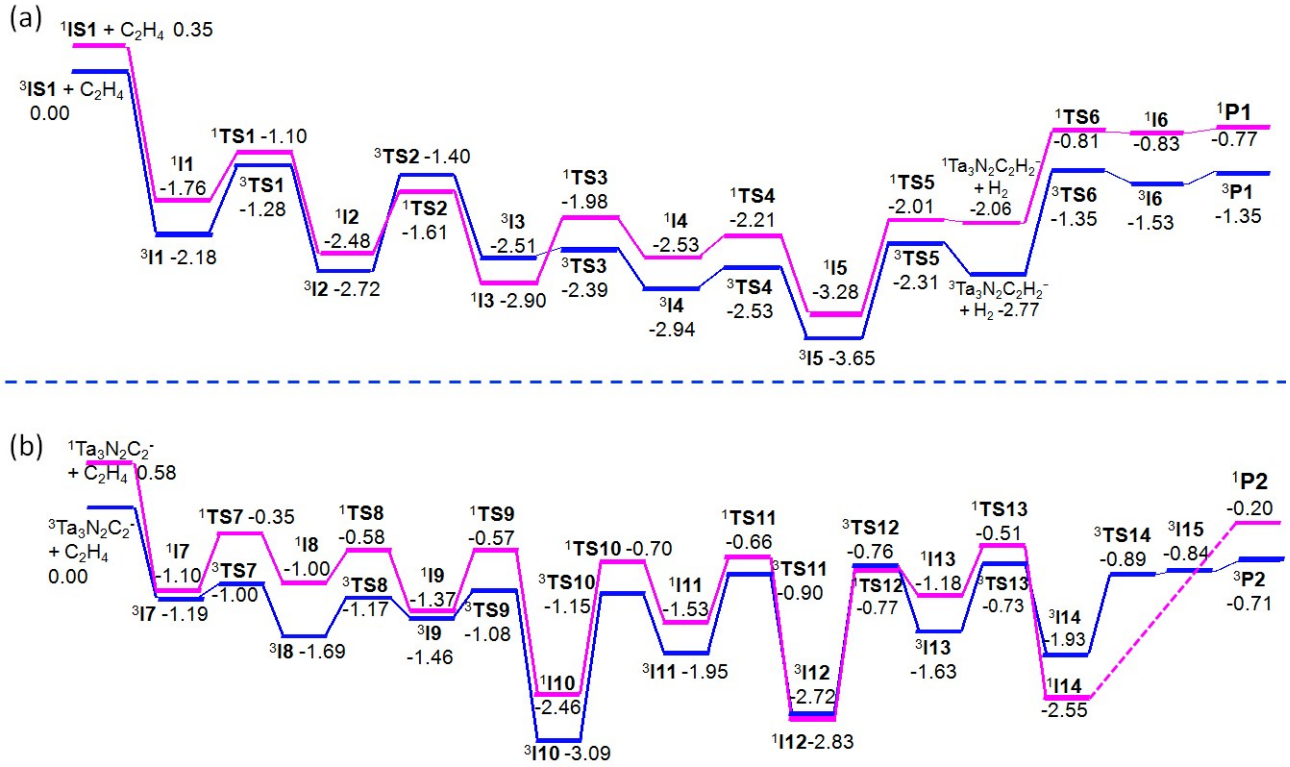

Fig. S5: DFT calculated PESs for the reactions of $Ta_3N_2^-$ and $Ta_3N_2C_2^-$ with C_2H_4. The zero-point vibration corrected energies (ΔH_{0K} in eV) of the reaction intermediates, transition states, and products with respect to the separated reactants are given. The superscripts indicate the spin states of species. The structures of singlet intermediates and transition states are not shown herein, which are similar to those on triplet potential energy surface. The singlet ^{1}**TS14** and ^{1}**I15** cannot be located on the PES.

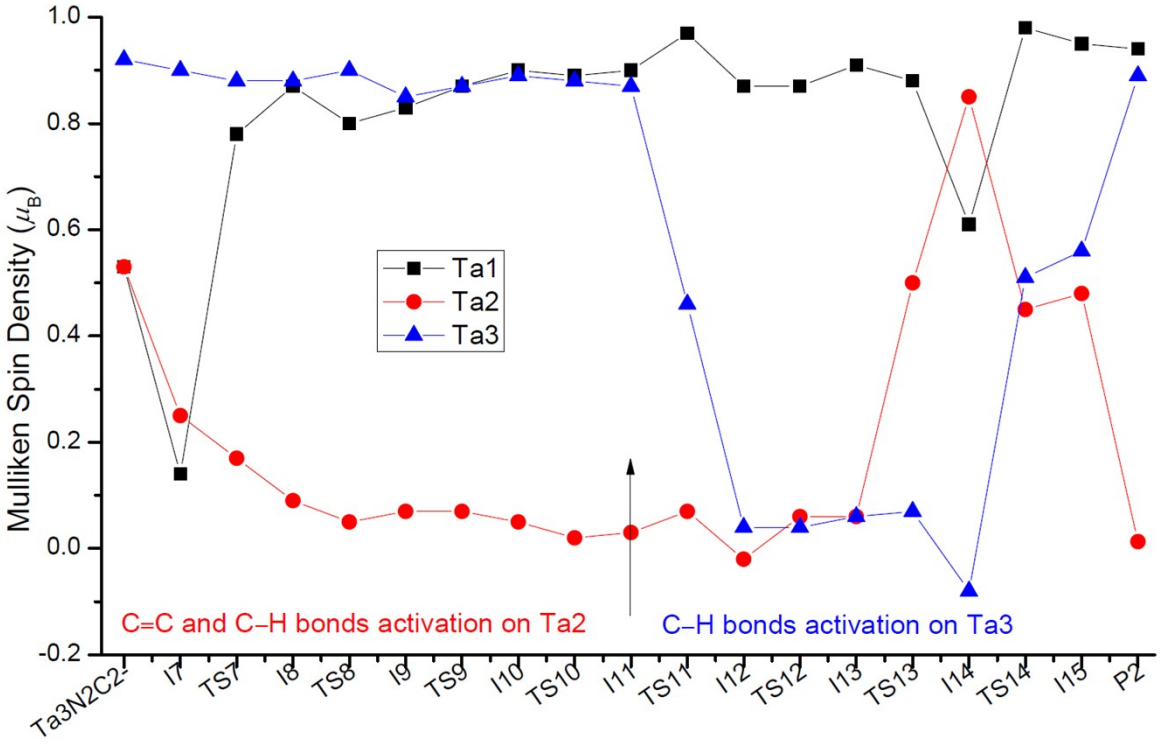

Fig. S6: DFT calculated Mulliken spin densities (in parentheses with unit of μ_B) on Ta1-Ta3 atoms along the reaction pathway of $Ta_3N_2C_2^-$ with C_2H_4 shown in Fig. 4 of the main text.

References

1 W. Xue, Z.-C. Wang, S.-G. He, Y. Xie, E. R. Bernstein, *J. Am. Chem. Soc.* 2008, **130**, 15879-15888.

2 Z. Yuan, Z.-Y. Li, Z.-X. Zhou, Q.-Y. Liu, Y.-X. Zhao, S.-G. He, *J. Phys. Chem. C* 2014, **118**, 14967-14976.

3 a) T. M. Bernhardt, *Int. J. Mass Spectrom.* 2005, **243**, 1-29; b) Y.-X. Zhao, Z.-Y. Li, Z. Yuan, X.-N. Li, S.-G. He, *Angew. Chem. Int. Ed.* 2014, **53**, 9482-9486.

4 D. R. Lide, *CRC Handbook of Chemistry and Physics*, 84th ed., CRC Press Inc., Boca Raton, FL, **2003**.